Available online at www.sciencedirect.com

jmr&t Journal of Materials Research and Technology

journal homepage: www.elsevier.com/locate/jmrt

Original Article

Impact of drying process on kraft lignin: lignin-water interaction mechanism study by 2D NIR correlation spectroscopy

Oihana Gordobil [a,*], *René Herrera* [a,b], *Faksawat Poohphajai* [a,c], *Jakub Sandak* [a,d], *Anna Sandak* [a,e]

[a] *InnoRenew CoE, Livade 6, 6310, Izola, Slovenia*
[b] *Department of Chemical and Environmental Engineering, University of the Basque Country, Plaza Europa, 1, 20018, Donostia-San Sebastián, Spain*
[c] *Aalto University School of Chemical Engineering, Department of Bioproducts and Biosystems, P.O.Box 16300, 00076, Aalto, Finland*
[d] *University of Primorska, Andrej Marušič Institute, 6000, Koper, Slovenia*
[e] *University of Primorska, Faculty of Mathematics, Natural Sciences and Information Technologies, Glagoljaška 8, 6000 Koper, Slovenia*

ARTICLE INFO

Article history:
Received 2 November 2020
Accepted 21 February 2021
Available online 25 February 2021

Keywords:
Hardwood kraft lignin
Drying temperature
DVS
NIR spectroscopy
2D-COS

ABSTRACT

Kraft lignin, an industrially available by-product from the pulp and paper industry, has revealed enormous potential to be valorised into a wide range of chemicals and biomaterials in the last two decades. However, the understanding of lignin chemistry remains challenging due to its chemical complexity. The goal of this work was to investigate the effect of drying temperature on the chemical, physical, and hygroscopic properties of hardwood kraft lignin isolated from industrial black liquor and elucidate the molecular interactions occurring between water and kraft lignin. Sorption-desorption isotherms determined by dynamic vapour sorption (DVS) technique revealed that the drying process considerably affected the hygroscopicity of the lignin polymer. Moreover, analytical pyrolysis (Py–GC–MS), dynamic NIR spectra collected as a function of relative humidity (0–95%) during sorption-desorption cycles and principal component analysis (PCA), evidenced chemical differences between lignin dried at room (25 °C) temperature and mild oven (55 °C) conditions. The main spectral changes associated with the water sorption in kraft lignin samples were analyzed using difference spectrum technique. 2D NIR spectral correlation analysis provided water sorption mechanism of lignin polymer, disclosing for the first time the sequential order in which water vapour molecules interact with active sorption sites in kraft lignin.

* Corresponding author.
E-mail address: oihana.gordobil@innorenew.eu (O. Gordobil).
https://doi.org/10.1016/j.jmrt.2021.02.080

1. Introduction

Lignin is the only high-molecular-weight renewable polyaromatic compound present in nature representing 10–35% of the lignocellulosic biomass. Lignin polymer is industrially available since it is produced as a by-product by the wood pulping industry. Nowadays, the kraft-pulping process is the most widespread method for pulp manufacture worldwide, managing around 85% of the market and producing annually more than 50 million tons of kraft lignin [1]. Despite the promising potential of kraft lignin as a feedstock to be valorised into chemicals [2], polymers [1,3,4], and, more recently, materials for food, biomedical, and pharmaceutical applications [5,6], most of the generated black liquor is still combusted as a low-value fuel for the production of heat and electricity as a part of the pulping process. Recently, in order to diversify their products portfolio, pulp and paper mills proposed the recovery and commercialization of kraft lignin. It is expected that this approach will increase their economic profit as well as improve their environmental profile through promoting sustainable products from a residual waste [7]. In the last two decades, several mills such as Mead-Westvaco (Canada), Nordic Paper Bäckhammer (Sweden), Domtar Plymouth Mill in North Carolina (USA), and Stora Enso (Finland) have made the effort to integrate a lignin recovery process in their mills. Nevertheless, the application of kraft lignin at large-scale still represents a big challenge. The chemical variability and complex structure of this abundant natural polymer are among the main factors that hamper its use in biorefineries and make difficult the development of optimized conversion processes for the obtention of lignin-derived high-value products [8]. Additionally, the typical dark colour of kraft lignin is presented as an aesthetical hindrance with important impact on the physical characteristics of the lignin-based products [9]. Although the valorisation of lignin for several application fields is a relevant topic of research, fundamental science about this complex polymer is still unknown. For instance, the hygroscopic properties of kraft lignin and its molecular interaction mechanism with water vapour in the environment. The hygroscopic character of lignin polymer, caused by the presence of many hydrophilic functional groups such as hydroxyl (phenolic and aliphatic), methoxyl, carbonyl, and carboxyl in its chemical structure, can greatly affect the final performance and stability of lignin-based products in particular applications [10]. Therefore, the study of moisture sorption–desorption properties of lignin polymer is essential for the understanding of lignin chemistry and its behaviour in changing environments. Dynamic vapour sorption (DVS) analysis is considered a useful technique for the determination of sorption isotherms of materials providing numerous advantages in comparison with a traditional static method [11,12]. The ultra-sensitive microbalance of this equipment requires a small sample mass for the measurement, which reduces the data acquisition time as well as offers an accurate determination of isotherms at different temperatures and over a wide range of relative humidity (0–95%). Volcova et al., 2012 [10], studied water sorption properties of Eucalyptus kraft lignin and lignin-based composites using a DVS apparatus. However, the information provided by DVS analysis was not enough to comprehend the water sorption process of this heterogeneous polymer. Several works have demonstrated the suitability of infrared spectroscopy for the study of the water vapour sorption mechanism of wood [13] and wood-derived materials like natural fibers [14] and cellulose [15]. This technique is based on the measurement of molecular vibrations as a result of the energy–matter interaction. Recently, Gou and co-workers, 2019 [16], investigated the adsorption of water molecules by polar groups present in commercial alkali lignin (Sigma Aldrich) using micro-FTIR spectroscopy during a water sorption cycle, recognizing carbonyl and hydroxyl groups as water sorption sites and describing the molecular association of adsorbed water with lignin. Mid-infrared spectroscopy investigates the fundamental vibrations of molecules ($v = 0$ to $v = 1$), whereas near-infrared, which is more energetic radiation, provides information on molecular overtones ($v = 0$ to $v > 1$) and combinations of vibrations [13]. To the best or our knowledge, no previous works have been found related to the study of water sorption mechanism of kraft lignin polymer using NIR technology, which greatly contributes insights into lignin chemistry where more complex molecular transitions occurs. Moreover, the NIR region has explicit absorption bands related to water interaction with materials, allowing assessment and monitoring of material affinity related to moisture changes. The goal of this research was to elucidate the water sorption mechanism of hardwood kraft lignin isolated from industrial black liquor as well as to reveal NIR bands of kraft lignin associated with the molecular sites capable of establishing hydrogen-bonds with water molecules during a sorption process. Molecular interactions occurring between water and lignin polymer have been studied using near-infrared (NIR) spectroscopy combined with principal component analysis (PCA) and 2D spectral correlations analysis. Moreover, the effect of the drying temperature on the physical, chemical, and hygroscopic properties has been evaluated.

2. Materials and methods

2.1. *Kraft lignin isolation*

Hardwood kraft lignin was isolated from industrial black liquor generated during the manufacturing of cellulose pulp from Eucalyptus chips. The precipitation was carried out using sulfuric acid (98%) as acidifying agent and lowering the pH of the supplied black liquor (initial pH~13) to pH 2. The lignin content of the supplied black liquor was 32 g/L. Then, precipitated lignin was recollected by filtration, washed until neutral pH and dried at controlled room conditions (25 °C) and in an oven using mild temperature (55 °C). Each resulted lignin was manually ground with a mortar and stored for further analysis.

2.2. *Molecular characteristics*

The weight-average (Mw), number-average (Mn), and polydispersity (Mw/Mn) of each kraft lignin were determined by Gel Permeation Chromatography (Jasco LCNet II/ADC), equipped with a refractive index detector (RI-2031 Plus

Intelligent), PolarGel-M column (300 mm 7.5 mm), and PolarGel-M guard (50 mm 7.5 mm). The column operated at 40 °C and eluted with N,N dimethylformamide (DMF) with 0.1% lithium bromide at flow of 0.7 mL/min. Polystyrene (Sigma–Aldrich) was used as a standard (70,000–266 g/mol). Lignin samples were also characterized by pyrolysis–gas chromatography–mass spectroscopy (Py–GC–MS) using a CDS Pyroprobe® model 5150 pyrolyzer. Identification of the pyrolysis products was accomplished using a GC–MS instrument (Agilent Techs. Inc. 6890 GC/5973MSD). The compounds were identified by comparing their mass spectra with the National Institute of Standards Library (NIST) and compounds reported in the literature [17–22]. A quantity between 400 and 800 mg was pyrolyzed in a quartz boat at 600 °C for 15 s with a heating rate of 20 °C/ms (ramp-off) with the interface kept at 260 °C. The pyrolyzates were purged from the pyrolysis interface into the GC injector under inert conditions using helium gas. The fused-silica capillary column used was an Equity-1701 (30 m × 0.20 mm × 0.25 μm). The GC oven program started at 50 °C and was held for 2 min. Then it was raised to 120 °C at 10 °C/min and was held for 5 min; after that, raised to 280 °C at 10 °C/min and was held for 8 min, and finally raised to 300 °C at 10 °C/min and was held for 10 min. Both GPC and analytical pyrolysis measurements were carried out in triplicate for each lignin sample. In addition, GPC results were analyzed with an ANOVA test and the software used was Origin 2017 (OriginLab Corporation, Northampton, MA, USA).

2.3. Visual appearance

The micromorphology of two hardwood kraft lignin samples was observed by using a digital microscope (Keyence, VHX-6000) at magnification of 500X with Epi-illumination light mode.

2.4. Moisture content measurements

Water sorption and desorption isotherms of kraft lignin dried at 25 °C (KL25) and 55 °C (KL55) were obtained using a dynamic vapour sorption apparatus (DVS-Surface Measurement Systems). An optimized condition, lowering weight change per minute (dm/dt) were set to obtain repeatable and reliable results. Each adsorption–desorption experiment took about 3 days and the humidity and temperature values were very stable during the tests. Lignin sample (10–20 mg) was placed on an aluminium plate connected to an ultra-sensitive microbalance capable of recording mass changes at a resolution of 0.1 μg, at established sorption-desorption conditions. Prior to sorption measurements, lignin samples were stabilized at 30 °C and 0% RH until weight change per minute (dm/dt) value reached 0.01%. This mass value was taken as dry mass reference value. Then, lignin sample was subjected to a gradual increase of relative humidity (20, 40, 60, 80, and 95% RH), followed by a sequential reduction to 0% RH. In order to ensure that the equilibrium moisture content (EMC) of lignin sample was reached at each RH condition, the instrument maintained a sample at a constant RH until the weight change per minute fell below 0.002% (dm/dt = 0.002).

2.5. Near infrared spectroscopy study

2.5.1. NIR spectra acquisition

Near infrared spectral measurements were performed in a Bruker MPA II spectrophotometer equipped with an integrating sphere accessory. NIR spectrum of lignin sample was recorded on diffuse reflectance mode from an average of 64 scans over the range 12,000–4000 cm^{-1} at a spectral resolution of 8 cm^{-1}. NIR spectra of each isolated kraft lignin was collected at different relative humidity (0, 35, 75, and 95%) at constant temperature (25 °C) during the sorption-desorption cycle. First, lignin samples were placed in a glass vials and freeze-dried for 24 h to remove the moisture content. Then, each lignin was conditioned in a sealed container at different relative humidity (0, 35, 75, and 95%) at constant temperature using saturated salt/water solutions (MgCl, NaCl and water). The equilibrium mass change and moisture content were gravimetrically measured at each relative humidity. Three independent measurements were performed on each sample.

2.5.2. Data processing

Firstly, extended multiplicative scatter correction (EMSC) was applied to the three measured spectra in each sample conditioning scenario in order to minimize an effect of uneven light scatter. Such corrected set of spectra was then averaged to determine the most representative single spectrum corresponding to each stage of RH. All the spectra were then used for determination of the dynamic response of each studied lignin to changing environmental conditions by interpolating these along the whole RH range from 0 to 100%. A polynomial (3rd degree) fitting algorithm was used, and the interpolation was performed independently for each spectral wavelength. In addition, NIR difference spectrum technique was applied by subtracting the spectrum measured at 0% RH to the interpolated spectra. This technique is useful to identify the main spectral region closely associated with water sorption in lignin. The second derivative spectra were calculated by an average of 100 points based on Savitzky–Golay method. Principal components analysis (PCA) was performed on that data set in order to identify clustering of samples according to their moisture content. These principal components can be segregated into those that represent useful information and those that represent irrelevant information or noise, thus reducing the effective dimensionality of the data. The software used for spectra processing and analysis, including EMSC, averaging as well as PCA, was PLS_Toolbox (Eigenvector Inc, USA), available as an extension of the Matlab package (Mathworks, USA).

2.5.3. Two-dimensional correlation spectroscopy (2D-COS)

2D NIR correlation analysis of dynamic spectra enables the study of molecular-level changes induced by an external perturbation. NIR spectra of kraft lignin samples exposed to different relative humidity conditions (0, 35, 75, and 95%) at constant temperature (25 °C) were collected and interpolated to obtain a representative dynamic spectra from 0 to 100% relative humidity. The cross-correlation analysis provides two different correlation maps. The synchronous and asynchronous correlation intensities formally correspond to the real

and imaginary part of the complex cross correlation function calculated along the variable t (external perturbation) between two spectral signal variations measured at wave numbers ν_1 and ν_2 [23]. 2D spectral correlation was performed with a custom software developed in LabView 2019 (National Instruments Inc, USA) implementing algorithms of Noda and Ozaki [23].

3. Results and discussion

3.1. Molecular characteristics

Gel permeation chromatography and analytical pyrolysis were used to investigate structural differences between kraft lignin dried at different temperatures. The precipitation step from black liquor was identical for each studied kraft lignin, the drying step being the only difference between them. Based on the results of GPC, no statistical differences were noticed with regard to the molecular weight distribution of each isolated kraft lignin (Table 1). The low molecular weight of hardwood kraft lignin results from the industrial process from which it comes, where degradation of β-aryl ether linkages in the lignin structure takes place during pulping bleaching [24]. Additionally, the chemical nature of hardwood lignin with high syringyl units as a structural element, partially avoid condensation reactions (5-5′and β-5′bonds) during the last stage of the process [25]. Furthermore, volatile fragments like phenolic compounds released during the thermal degradation of lignin in the absence of oxygen provide useful structural information about chemical characteristics of the macromolecule. In this study, 33 phenolic-derived compounds, which represent 88–90% of total area, were identified and classified according to their aromatic structure and origin: phenol-type compounds (H), guaiacyl-type compounds (G), syringyl-type compounds (S), and catechol-type compounds (Ca). During fast pyrolysis, some differences regarding released compounds between lignin samples were observed. Although syringyl and guaiacyl-type compounds were dominant in both pyrograms, significant area percentage of catechol-type compounds was also detected (8–10%). These compounds are usually produced from demethoxylation (Ph-OCH_3 cracking) and demethylation (PhO-CH_3 cracking) of S-type compounds generating phenol derivatives and catechol-type compounds, respectively [26]. Therefore, even though similar relative content of methoxylated phenolic groups were detected during analytical pyrolysis for each kraft lignin, 73% and 80% of these compounds came from S-type compounds for KL25 and KL55, respectively. Furthermore, several differences were observed by sorting the released lignin-derived aromatic products according to the structural characteristic of their side chain (Table 1). The major difference between kraft lignins corresponded to the amount of released phenolic compounds with a side chain attached to the aromatic ring. The content of phenolic compounds with short and long side chains (non-substituted and substituted) was found to be higher for KL55 than for KL25. The presence of lignin-derived compounds with non-substituted saturated side chains, such as 4-methylguaiacol, 4-ethylguaiacol, 4-propylguaiacol, 4-methylsyringol, 4-ethylsyringol, and 4-propylsiringol, was more abundant in oven-dried kraft lignin (KL55) than in the pyrogram of kraft lignin dried at room temperature (KL25). In addition, the content of phenolic compounds with unsaturated side chains, such as vinylsyrirngol, vinylguaiacol, isoeugenol, and allylsyringol was found higher for KL55 than KL25. Regarding the phenolic derivatives with oxidized structures in the side chain (aldehydes and ketones), no relevant differences were noticed between isolated kraft lignins.

Table 1 – Molecular weight distributions and relative content (%) of phenolic compounds released during fast pyrolysis of kraft lignins.

	KL25	KL55
Mn	669 ± 18[d]	683 ± 24[d]
Mw	2477 ± 132[d]	2285 ± 173[d]
IP	3.7	3.3
H-type	2.1 ± 0.6	1.9 ± 0.1
Ca-type	9.3 ± 0.3	8.0 ± 0.7
G-type	24.9 ± 4.6	16.8 ± 1.7
S-type	52.0 ± 8.3	63.8 ± 0.5
Methoxylated phenolic groups (%)[a]	86.3 ± 3.9	88.2 ± 2.1
Non-substituted saturated chains (%)[b]	28.3 ± 1.0	38.8 ± 5.0
Unsaturated side chains (C=C) (%)[c]	6.7 ± 0.2	10.2 ± 0.5
Oxygenated groups in the side chains (C=O) (%)	2.5 ± 1.3	2.1 ± 0.2
Short side chain (C_1+C_2)	34.9 ± 0.3	47.3 ± 5.2
Long side chain (C_3)	3.0 ± 1.4	5.3 ± 1.9

[a] Guaiacyl and syringyl-type compounds.
[b] Short and propanoid side chains attached to the aromatic ring.
[c] Compounds with unsaturations in $C_\alpha = C_\beta$ and $C_\beta = C_\gamma$ positions.
[d] The population means are not significantly different at the 0.05 level according to the one way analysis of variance (ANOVA).

3.2. Physical characteristics

Fig. 1 presents a clear effect of the drying step on the morphological properties and colour of kraft lignin. The procedure followed for obtention of each kraft lignin from industrial black liquor resulted in a powder formed by lignin particles of irregular size and no uniform shape. However, significant differences regarding the colour and morphological aspects between the two kraft lignin were observed. Oven-dried kraft lignin (KL55) presented smooth dark surface particles with caramel appearance, due to the burning effect during drying, that were covered by smaller and lighter particles. Conversely, KL25 exhibited as non-uniform shape clods covered by smaller lignin particles aggregated closely, forming a rough surface texture.

Although, KL55 also presented small light particles on its surface, in KL25, a larger amount of smaller lignin particles than in KL55 were observed. Zhang et al., 2018 [27], also proved that drying procedures in the presence of temperature generate dark lignin with smooth surfaces, while the absence of temperature produces lighter colour lignin with smaller particle sizes. Lignin is naturally a rigid and brittle polymer due to its amorphous, highly cross-linked structure and strong intermolecular hydrogen bonding interactions, which restrict thermal mobility of the chemical structure. Glass transition temperature (T_g) for hardwood kraft lignin in the literature

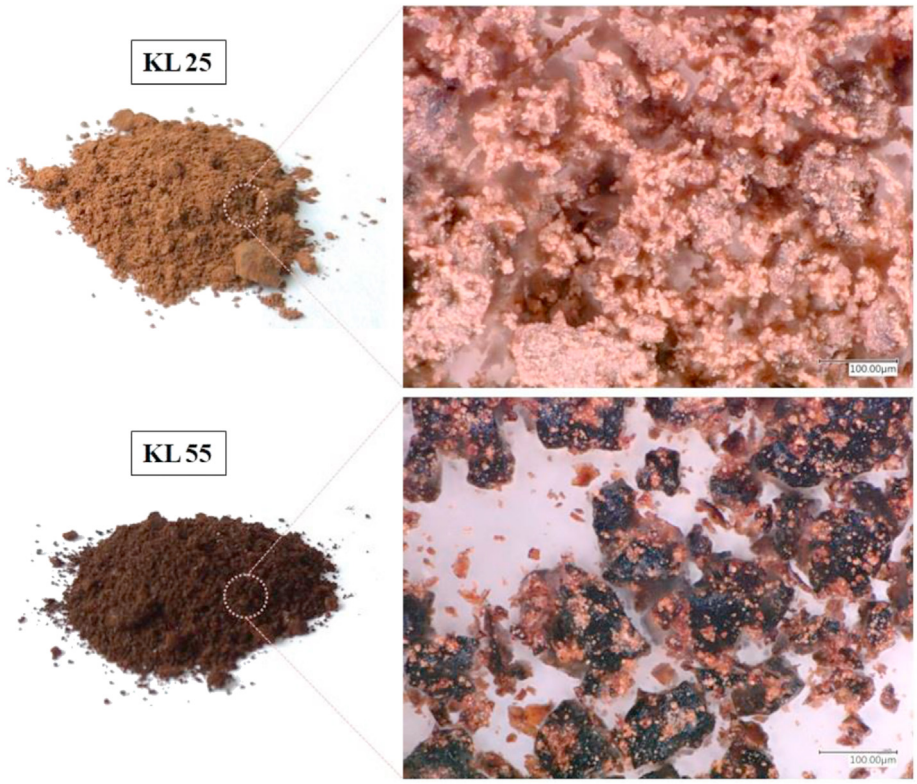

Fig. 1 – Hardwood kraft lignin dried at room temperature (25 °C) and dried in mild oven conditions (55 °C).

was found between 115 and 125 °C [28]. However, T_g of lignin polymer is greatly affected by moisture content, decreasing up to 50 °C at high moisture content, as was previously reported by Morsing, 1998 [29]. Hence, the colour and morphological differences between studied samples were associated with the drying step, which occurred below T_g for KL25 and over T_g in KL55. The drying of lignin at temperatures over its glass transition in wet state (after precipitation and washing) originated a particular caramel-like appearance of particles in KL55.

3.3. *Hygroscopic properties of kraft lignin*

Hygroscopicity of lignin is an important aspect to consider and control, especially for development of high-performance applications. Rawat and Khali, 1990 [30], reported the first research paper about adsorption of water vapour in lignin, where the adsorption mechanism was validated by Brunauer, Emmett and Teller (BET) theory. However, since then the hygroscopic behaviour of lignin polymer has been an unexplored topic. Therefore, the present work studied water vapour sorption properties of industrially produced hardwood kraft lignin using a dynamic vapour sorption analysis in the 0–95% relative humidity range at constant temperature (25 °C). Additionally, the effect of drying process on hygroscopic properties was investigated. Equilibrium moisture content during a sorption-desorption cycle of kraft lignin samples is presented in Fig. 2. According to the IUPAC isotherms classifications [31] and previous reported studies [11,32], kraft lignin exhibited sigmoid shape isotherms (type II). As a result of the monolayer-multilayer adsorption mechanism, type II isotherms are concave at low RH%, approximately linear in the intermediate region, and convex at high RH% [17]. This type of isotherm is commonly found in wood and wood-derived compounds (macroporous materials). Nevertheless, as can be observed in Fig. 2, the hygroscopic property of isolated kraft lignin was highly affected by drying temperature. KL25 dried at room temperature reached up to 21% of moisture content at 95% relative humidity, while the maximum water content in KL55 dried at 55 °C in saturated conditions was around 10%. Moreover, a gradual water sorption was observed for KL55, while in the case of KL25, around 50% of the total adsorbed water occurred at high RH (above 80%). The different hygroscopic pattern of each kraft lignin could be explained by the following theory. According to previously reported studies, when a hygroscopic material undergoes the drying process, an irreversible hydrogen bond formation can take place, resulting in a reduced availability of sorption sites to bond with the water vapour molecules during a sorption cycle [11,18,19]. Thus, the lower affinity of KL55 toward water vapour was associated with this phenomenon. In addition, a hysteresis phenomenon is clearly visible in each kraft lignin. Hysteresis is expressed by the difference between equilibrium moisture content in sorption and desorption at the same relative humidity. Oven-dried kraft lignin (KL55) presented higher hysteresis than kraft lignin dried at room temperature (KL25), especially at relative humidity lower than 60%. These results indicated the lower capacity of KL55 to release the adsorbed water during a desorption process. In contrast, KL25 had the capacity to reach initial equilibrium moisture content during

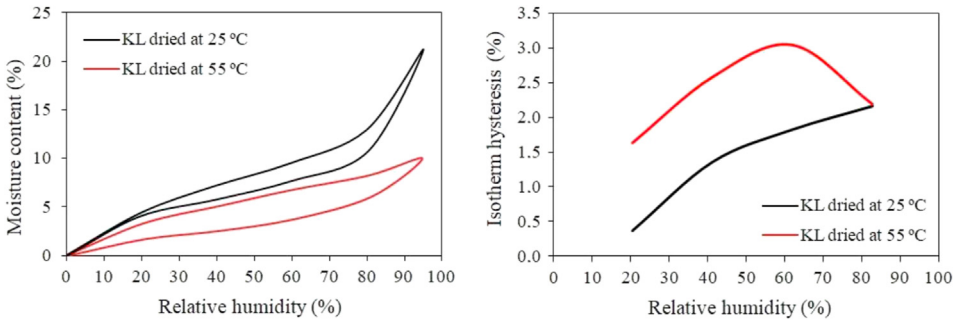

Fig. 2 – Experimental sorption-desorption isotherms determined by DVS technique and hysteresis of kraft lignin dried at 25 °C and 55 °C.

the desorption cycle at lower RH% (<20%), suggesting its ability to recover the original state. Although, several theories have been reported regarding the hysteresis phenomenon in wood, the explanation of this irreversible event in lignin is not fully understood. As a heterogeneous polymer, lignin hygroscopicity may be influenced by several factors since water sorption sites are not only dependent on the chemical structure but also on the microstructure of the material [11,20]. The morphological differences between lignin due to drying conditions could explain the differences observed from the hysteresis phenomenon, which is widely related to the microstructures of the material [21,22]. Relying on reported theories, the micromorphology of KL55 hinders easy release of absorbed water during desorption, while the microstructure features of KL25 enables recovering of the initial equilibrium moisture content at 20% RH. Moreover, the particular sorption capacity of KL25 occurred above 80% RH, allows the sorption of water bonded to a previously adsorbed water molecule forming strong hydrogen bonds, as was previously reported [16,32]. This phenomenon is hardly visible in KL55, probably due to the steric hindrance of the microstructure.

3.4. *Near infrared spectroscopy study*

3.4.1. *Absorbance bands of NIR spectra related to lignin-water interactions*

The exposure of lignin samples to an external perturbation, such as different relative humidity conditions, induced molecular-level changes that generated spectral variations such as intensity changes, band shifts or change in the band shapes [23]. With the goal of identifying the main spectral changes associated with water sorption in kraft lignin samples, difference spectrum technique was applied. The variation observed in specific spectral ranges is related to the functional groups of lignin affected by the moisture uptake. Fig. 3, which was represented using the same scale on the y-axis, shows NIR spectra difference of KL25 and KL55 during the sorption cycle. Although major changes corresponded to intensity changes, band shifts were also detected during water adsorption process. The moisture absorption of studied lignin samples involved changes in the same spectral ranges; however, spectral variations were affected following different trends for each lignin type. The spectral range above 7500 cm^{-1} has been previously related to colour and particle size [33]. The dark colour of wood samples results in higher infrared light absorbance in this region as was reported by Mitsui et al., 2008 [34]. However, decrease of absorbance can be observed with increased relative humidity. This reduction was especially obvious in the range of 8300–8800 cm^{-1} for KL55, which is associated with methyl groups in aromatic structures (2nd OT C–H stretching $-CH_3$) and 2nd OT asymmetric stretching of C–H and HC=CH of lignin [35,36]. Methoxyls (auxochromes) and carbon–carbon double bonds (chromophores) are functional groups responsible for the dark colour of lignin polymer. Furthermore, with an increase in RH, spectral changes in the region 6000-7500 cm^{-1} were clearly

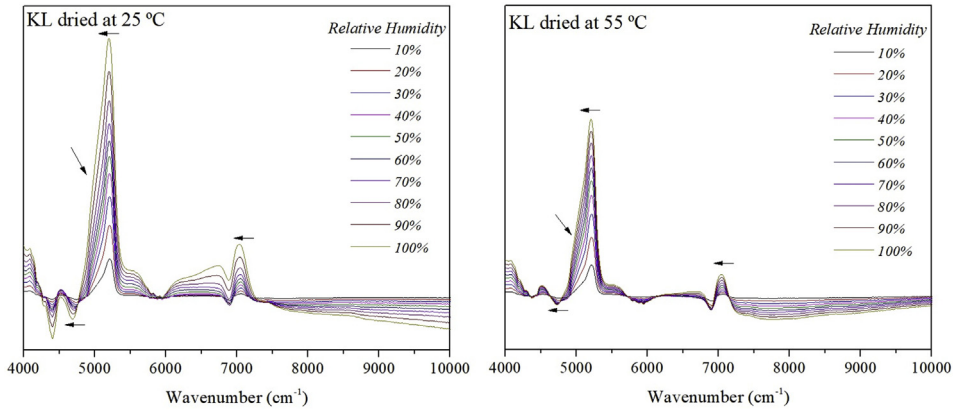

Fig. 3 – Dynamic spectra of kraft lignin (KL25 and KL55) under different relative humidity (sorption cycle).

noticeable, especially for KL25. Different spectral response between each lignin indicated that KL25 contains more available sorption sites than KL55. This spectral range is associated with hydroxyl groups of lignin polymer (1st OT of different O–H stretching vibrations) [33,37] and C–H deformation of methyl groups in acetyl esters of lignin (7400 cm^{-1}) [33]. With regard to the band at 7070 cm^{-1}, which corresponds to the 1st OT of O–H stretching of phenolic hydroxyl groups present in lignin, a shift to lower wavenumbers (7050 cm^{-1}) was observed due to the interaction with water molecules and formation of water–water weak hydrogen bonds [38,39]. This trend was more perceptible in KL25, and the band shift was significantly appreciable at RH above 80%. Fig. 4 shows the growth trends of the most affected bands as a function of relative humidity. As can be observed, increasing intensity of the band located at 7050 cm^{-1} was more gradual in KL55, while in KL25, slope of the line was considerably increased when relative humidity was higher than 80%. These results agree with the isotherm of KL25, where most of the absorbed water occurred above 80% RH. The band at 6915 cm^{-1} (phenolic hydroxyl groups) [34] had two spectral variations such as intensity change and band shift to 6890 cm^{-1}, which reflected the presence of phenolic groups with intramolecular hydrogen bonds [33]. Moreover, in KL25, an increase of two broad bands (6750 cm^{-1} and 6190 cm^{-1}) within the relative humidity can be observed; but these were practically constant in the case of KL55. In the literature, these bands were only associated with 1st OT O–H stretching in weakly H-bonded hydroxyls of cellulose and water [38,40]. However, this range of near infrared is also clearly related to phenolic groups of lignin compound and its interaction with water vapour. Fig. 4 presents a clear different response of kraft lignin for these bands against RH%. Moreover, the absorption at 5940 cm^{-1} (1st OT C_{ar}-H stretching) associated with an aromatic skeletal of lignin [34,41], 5880 cm^{-1} (1st OT of aliphatic C–H stretching) [41] and 5790 cm^{-1} (1st OT C–H stretching of $-CH_2$ groups), remained unchanged for KL25. Conversely, a clear reduction in KL55 spectra was found. The spectral response of these bands associated with aliphatic side chains of aromatic structures in the case of KL55 suggests the major contribution of these structural moieties in its chemical structure. Near infrared absorption spectra from 5500 to 4800 cm^{-1} is highly overlapped but totally dominated by water (combination of O–H stretching and deformation vibrations) [33]. In this region an important peak (water band) with maximum around 5200 cm^{-1} was observed for each lignin. The water band clearly increased and shifted to lower wavenumbers with increasing moisture content in lignin. Moreover, this band shape changed with the appearance of overlapped peak as revealed by the second derivative at 4960 cm^{-1}, which was more noticeable in KL25. At higher wavenumbers (5700-5300 cm^{-1}), a band at 5390 cm^{-1} was also noticed. Although these spectral variations (intensity changes, band shift and shape change) were found in both lignin types, the changes were less intense for KL55 than those observed for KL25 (see Fig. 3). It is important to mention that the increase in moisture uptake occurring above 80% RH reflected by isotherms for KL25 was also evident in the NIR spectral changes. To lower wavenumbers, different trends were observed for each lignin type. The absorption band at 4700 cm^{-1} (C_{ar}-H and C=C stretching in lignin) [42] was reduced and shifted to lower wavenumbers with increasing moisture content. However, this trend was more noticeable for KL25. The subsequent band, located at 4520 cm^{-1} (C–H and C=O stretching in aromatic aldehydes) [35,41], clearly increased for KL55. The same peak, in the case of KL25, increased only slightly up to 70% RH. Finally, the band at 4400 cm^{-1} related to O–H and C–O stretching in lignin was practically constant in KL55 but strongly reduced for KL25.

3.4.2. *Exploratory analysis*

Firstly, the NIR spectra were pre-processed by applying extended multiplicative scatter correction (EMSC) and mean centering. The pre-processed data was evaluated by principal component analysis (PCA), reducing the spectroscopic data into an alternative presentation of variables such as scores and loadings. PCA was used to examine differences between isolated kraft lignin and identify the variables that contribute most to this differentiation. The PCA model described the spectral variance in the range of 7500–4200 cm^{-1} with three principal components (PCs) explaining 99.95% of the variance. As can be observed in Fig. 5, PC1 covers 96.79% of the spectral variance and clearly discriminates lignin samples according to the relative humidity to which they were exposed. Both KL25 and KL55 showed a negative score in PC1 at low RH%, while at high RH% samples were located in the positive side of PC1. Moreover, PC2, with only 2.03% of variance, was able to differentiate studied kraft lignin. The spectral group corresponding to oven-dried kraft lignin (KL55) showed a positive score in PC2 in contrast to kraft lignin dried at room temperature (KL25). Therefore, it can be stated that PC1 had information related to the interaction between lignin and water vapour, while PC2 reflects the chemical structure of studied lignin samples. The loading plots (Fig. 5) evidenced the

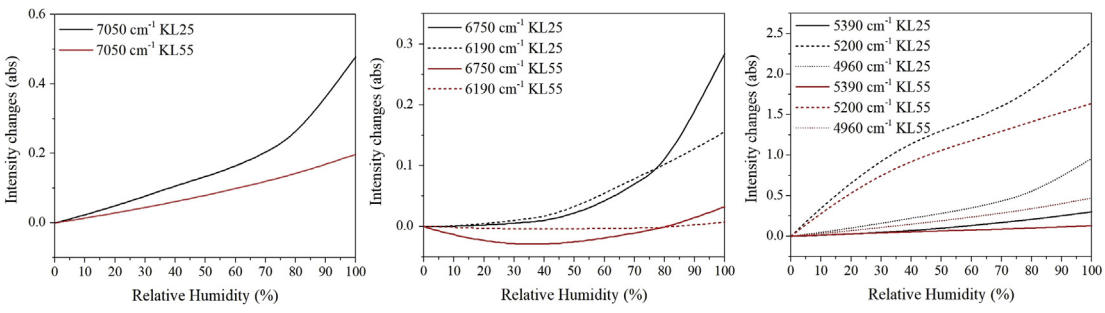

Fig. 4 – Intensity changes of NIR spectra bands affected by moisture sorption against RH.

importance of original variables (bands) that mostly contribute to the separation of lignin samples in each PC. The loadings of PC1 showed a high influence of the bands at 7050 and 5200 cm^{-1}, which are related to the interaction of phenolic hydroxyls groups with water molecules and the formation of water–water weak hydrogen bonds, respectively. However, the bands that most contribute to PC2 are associated with the chemical structure of lignin. For example, band at 6860 cm^{-1} corresponds to the intramolecular phenolic hydroxyl groups in lignin polymer. Positive scores of KL55 in PC2 suggest that the phenolic hydroxyl groups are linked through intramolecular H-bonds, indicating that chemical structure of kraft lignin was affected by the drying process. Moreover, bands at 5940, 5880, and 5790 cm^{-1} are related to the aromatic skeletal and C–H stretching of the aliphatic side chain. Additionally, the broad band between 5100 and 4500 cm^{-1} is correlated to the C=C and C=O functional groups present in the aliphatic side chain attached to the aromatic ring [35,42]. This is in agreement with the results from analytical pyrolysis, which demonstrated that the presence of lignin-derived compound with non-substituted saturated and unsaturated side chains were more abundant for KL55.

3.4.3. *Two-dimensional correlation spectroscopy (2D-COS)*

2D correlation analysis of dynamic spectra was used to study the specific water–lignin interactions and molecular-level responses of KL25 and KL55 induced by an external perturbation (changes in relative humidity of the environment). This technique, aside from evidencing the main spectral variations that took place during an external perturbation, allows study of the water–lignin interaction mechanism through examination of synchronous and asynchronous 2D correlation maps. Synchronous 2D correlation map represents simultaneous or coincidental changes of spectral intensity variations due to the external perturbation. It is a symmetrical matrix with respect to the main diagonal line corresponding to coordinates $\nu_1 = \nu_2$. Correlation peaks can appear both at diagonal (autopeaks) and off-diagonal (cross peaks) positions. Autopeaks, which are always positive, show the spectral regions that change because of the external perturbation, while cross-peaks reveal coincidental changes of two different intensity signals observed at coordinates ν_1 and ν_2 [43]. In contrast, asynchronous spectrum is related to the sequential or successive spectral changes and provides information about the order of spectral intensity changes along the perturbation, consisting exclusively of cross peaks located at off-diagonal positions [23]. In addition, the intensity of peaks on the autocorrelation spectrum is directly proportional to the relative importance of the intensity change in the original spectra. Fig. 6 shows synchronous and asynchronous 2D correlation map in the region from 6000 to 7500 cm^{-1}. In the synchronous 2D correlation spectrum for KL25, two autopeaks can be observed at the diagonal position at 7050 cm^{-1} (strong autopeak) and at 6750 cm^{-1} (weak autopeak). Both are related

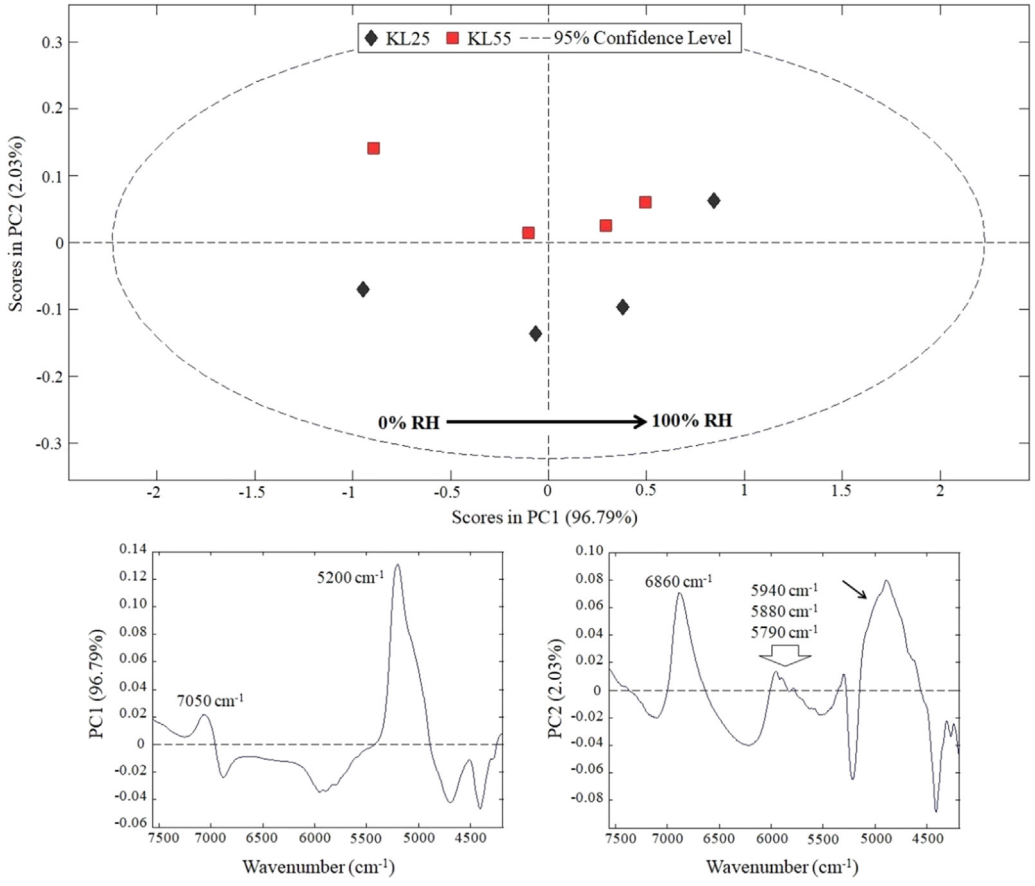

Fig. 5 – Scores plot in the plane of PC1 vs PC2 and loadings of PC1 and PC2.

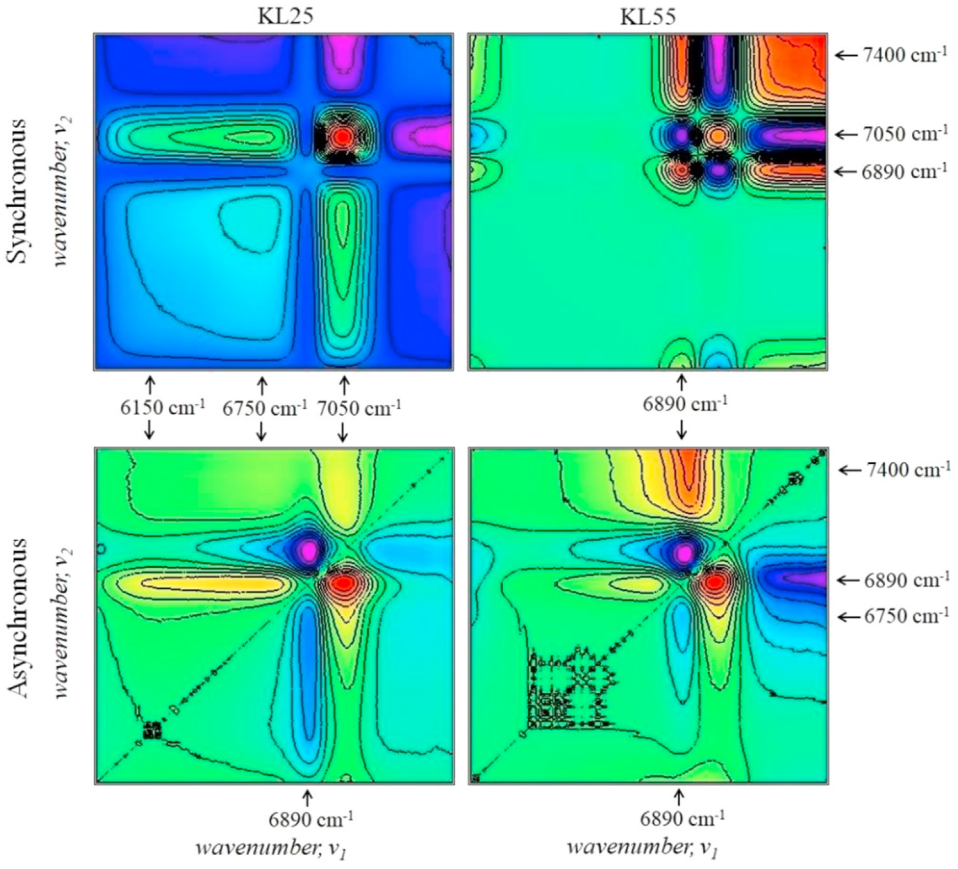

Fig. 6 – Synchronous and asynchronous 2D correlation maps in the 6000-7500 cm^{-1} region.

to the water sorption in phenolic hydroxyl groups of lignin compound. In addition, one cross peak centered at Φ(6750–7050)>0 was noticeable. Five bands were identified in the asynchronous 2D correlation spectrum at 6150, 6750, 6890, 7050, and 7400 cm^{-1}. These bands formed three positive cross peaks at Ψ(6150–6890)>0, Ψ(6750–6890)>0 and Ψ(7050–7400) >0 and a single negative at Ψ(6890–7050)<0. Therefore, based on Noda's fundamental rule of asynchronous spectrum [23], the following sequence of spectral intensity changes was determined: 7050 > 6750, 6150 > 6890>7400. However, the spectra of KL55 showed slightly different response to the relative humidity variations. In this case, an autopeak at 7050 cm^{-1} was evidenced, but noticeably less intense than in KL25. In addition, two more autopeaks at 6890 cm^{-1} and at 7400 cm^{-1} were observed. These bands represent the overall susceptibility of the spectral signal to change intensity when lignin is exposed to relative humidity variations. In addition two negative cross peaks at cross peak centered at Φ(6890–7050)<0 and Φ(7050–7400)<0 as well as one positive at Φ(6890–7400)>0 were identified. The asynchronous map revealed four bands located at 6750, 6890, 7050, and 7400 cm^{-1}. In this case, positive cross-peaks at Ψ(6750–6890)>0 and Ψ(6890–7400)>0 combined with one negative at Ψ(6890–7050) <0 were identified. It indicated the following sequence of spectral intensity changes: 7050 > 6750>6890 > 7400. Therefore, despite less availability of effective water sorption sites in KL55, it can be confirmed that lignin-water molecular interactions mechanism for each studied kraft lignin follows the same pattern. In both cases, the first functional groups that interact with water molecules are phenolic hydroxyl groups, followed by carbonyl groups.

4. Conclusion

In this work, the effect of drying temperature on hygroscopic properties of hardwood kraft lignin isolated from industrial black liquor was investigated using a DVS technique and NIR spectroscopy. The drying process had an impact on lignin structure, colour and micromorphology. Lignin-water molecular interaction mechanism was closely studied by analysing differential spectra, principal component analysis (PCA), and 2D NIR spectral correlation. It was demonstrated that the drying process considerably affected kraft lignin chemistry decreasing available water sorption sites and, consequently, moisture sorption capacity. KL dried in mild oven conditions (KL55) was less hygroscopic than KL dried at room conditions (KL25), due to less availability of accessible water sorption sites in the chemical structure of KL55, which was confirmed by NIR spectroscopy. Further quantitative analytical methods such as NMR could give an additional insight on this matter. In addition, the results from analytical pyrolysis and PCA analysis proved chemical differences between kraft lignin due to drying temperature. 2D-COS combined with NIR spectroscopy provided useful information about the molecular interactions occurring between water and isolated kraft lignin during

water sorption process. Aside from recognizing phenolic hydroxyl groups and carbonyl groups as active water sorption sites in lignin, this work revealed for the first time that the molecular association of adsorbed water in lignin polymer occurs first with phenolic hydroxyls groups, followed by carbonyl groups.

Declaration of Competing Interest

The authors declare that they have no known competing financial interests or personal relationships that could have appeared to influence the work reported in this paper.

Acknowledgements

The author gratefully acknowledges the European Commission for funding the InnoRenew project [Grant Agreement # 739574] under the Horizon 2020 Widespread-Teaming program, the Republic of Slovenia (investment funding from the Republic of Slovenia and the European Union European Regional Development Fund) and infrastructural ARRS program IO-0035. Part of this work was conducted during the project Multi-spec (BI-IT/18-20-007) funded by ARRS. Additionally, O.G. is grateful for the financial support received from the University of the Basque Country (post-doctoral grant of Ms. Gordobil DOCREC18/29) and R.H. acknowledges to the Department of Education of the Basque Government (post-doctoral grant).

REFERENCES

[1] Tribot A, Amer G, Abdou Alio M, de Baynast H, Delattre C, Pons A, et al. Wood-lignin: supply, extraction processes and use as bio-based material. Eur Polym J 2019. https://doi.org/10.1016/j.eurpolymj.2019.01.007.

[2] Schutyser W, Renders T, Van Den Bosch S, Koelewijn SF, Beckham GT, Sels BF. Chemicals from lignin: an interplay of lignocellulose fractionation, depolymerisation, and upgrading. Chem Soc Rev 2018. https://doi.org/10.1039/c7cs00566k.

[3] Laurichesse S, Huillet C, Avérous L. Original polyols based on organosolv lignin and fatty acids: new bio-based building blocks for segmented polyurethane synthesis. Green Chem 2014;16:3958–70. https://doi.org/10.1039/C4GC00596A.

[4] Li B, Yuan Z, Schmidt J, Xu C. New foaming formulations for production of bio-phenol formaldehyde foams using raw kraft lignin (Charles) Eur Polym J 2019. https://doi.org/10.1016/j.eurpolymj.2018.12.011.

[5] Spiridon I, Poni P, Chemistry M, Ghica G, Alley V. Biological and pharmaceutical applications of lignin and its Derivatives: a mini-review. Cellul Chem Technol 2018;52:543–50. https://doi.org/10.1016/S0142-9612(03)00314-4.

[6] Gil-Chávez J, Gurikov P, Hu X, Meyer R, Reynolds W, Smirnova I. Application of novel and technical lignins in food and pharmaceutical industries: structure-function relationship and current challenges. Biomass Convers Biorefinery 2019. https://doi.org/10.1007/s13399-019-00458-6.

[7] Välimäki E, Niemi P, Haaga K. A case study on the effects of lignin recovery on recovery boiler operation. In: 2010 Int. Chem. Recover. Conf., vol. 2; 2010. p. 148–59.

[8] Vishtal A, Kraslawski A. Challenges in industrial applications of technical lignins. BioResources 2011;6:3547–68. https://doi.org/10.15376/BIORES.6.3.3547-3568.

[9] Ajao O, Jeaidi J, Benali M, Restrepo AM, El Mehdi N, Boumghar Y. Quantification and variability analysis of lignin optical properties for colour-dependent industrial applications. Molecules 2018;23. https://doi.org/10.3390/molecules23020377.

[10] Volkova N, Ibrahim V, Hatti-Kaul R, Wadsö L. Water sorption isotherms of Kraft lignin and its composites. Carbohydr Polym 2012. https://doi.org/10.1016/j.carbpol.2011.10.001.

[11] Almeida G, Rémond R, Perré P. Hygroscopic behaviour of lignocellulosic materials: dataset at oscillating relative humidity variations. J Build Eng 2018. https://doi.org/10.1016/j.jobe.2018.05.005.

[12] Hill CAS, Norton A, Newman G. The water vapor sorption behavior of natural fibers. J Appl Polym Sci 2009. https://doi.org/10.1002/app.29725.

[13] Xu F, Yu J, Tesso T, Dowell F, Wang D. Qualitative and quantitative analysis of lignocellulosic biomass using infrared techniques: a mini-review. Appl Energy 2013. https://doi.org/10.1016/j.apenergy.2012.12.019.

[14] Célino A, Gonçalves O, Jacquemin F, Fréour S. Qualitative and quantitative assessment of water sorption in natural fibres using ATR-FTIR spectroscopy. Carbohydr Polym 2014. https://doi.org/10.1016/j.carbpol.2013.09.023.

[15] Olsson AM, Salmén L. The association of water to cellulose and hemicellulose in paper examined by FTIR spectroscopy. Carbohydr Res 2004. https://doi.org/10.1016/j.carres.2004.01.005.

[16] Guo X, Yuan H, Xiao T, Wu Y. Application of micro-FTIR spectroscopy to study molecular association of adsorbed water with lignin. Int J Biol Macromol 2019. https://doi.org/10.1016/j.ijbiomac.2019.03.193.

[17] Brunauer S, Emmett PH, Teller E. Adsorption of gases in multimolecular layers. J Am Chem Soc 1938. https://doi.org/10.1021/ja01269a023.

[18] Hill CAS, Norton AJ, Newman G. The water vapour sorption properties of Sitka spruce determined using a dynamic vapour sorption apparatus. Wood Sci Technol 2010. https://doi.org/10.1007/s00226-010-0305-y.

[19] Thybring EE, Thygesen LG, Burgert I. Hydroxyl accessibility in wood cell walls as affected by drying and re-wetting procedures. Cellulose 2017. https://doi.org/10.1007/s10570-017-1278-x.

[20] Uimonen T, Hautamäki S, Altgen M, Kymälaïnen M, Rautkari L. Dynamic vapour sorption protocols for the quantification of accessible hydroxyl groups in wood. Holzforschung 2020. https://doi.org/10.1515/hf-2019-0058.

[21] Ciolacu D, Doroftei F, Cazacu G, Cazacu M. Morphological and surface aspects of cellulose-lignin hydrogels. Cellul Chem Technol 2013.

[22] Vrentas JS, Vrentas CM. Hysteresis effects for sorption in glassy polymers. Macromolecules 1996. https://doi.org/10.1021/ma950969l.

[23] Noda I, Ozaki Y. Two-dimensional correlation spectroscopy - applications in vibrational and optical spectroscopy. 2005. https://doi.org/10.1002/0470012404.

[24] Yuan TQ, He J, Xu F, Sun RC. Fractionation and physico-chemical analysis of degraded lignins from the black liquor of Eucalyptus pellita KP-AQ pulping. Polym Degrad Stabil 2009;94:1142–50. https://doi.org/10.1016/j.polymdegradstab.2009.03.019.

[25] Holtman KM, Chang HM, Jameel H, Kadla JF. Quantitative 13C NMR characterization of milled wood lignins isolated by

different milling techniques. J Wood Chem Technol 2006;26:21–34. https://doi.org/10.1080/02773810600582152.
[26] Zhao J, Xiuwen W, Hu J, Liu Q, Shen D, Xiao R. Thermal degradation of softwood lignin and hardwood lignin by TG-FTIR and Py-GC/MS. Polym Degrad Stabil 2014;108:133–8. https://doi.org/10.1016/j.polymdegradstab.2014.06.006.
[27] Zhang H, Chen F, Liu X, Fu S. Micromorphology influence on the color performance of lignin and its application in guiding the preparation of light-colored lignin sunscreen. ACS Sustainable Chem Eng 2018. https://doi.org/10.1021/acssuschemeng.8b03464.
[28] Gordobil O, Delucis R, Egüés I, Labidi J. Kraft lignin as filler in PLA to improve ductility and thermal properties. Ind Crop Prod 2015;72:46–53. https://doi.org/10.1016/j.indcrop.2015.01.055.
[29] Morsing N. Densification of Wood.: the influence of hygrothermal treatment on compression of beech perpendicular to gain. 1998.
[30] Rawat SPS, Khali DP. Studies on adsorption behaviour of water vapour in lignin using the Brunauer-Emmett-Teller theory. Holz als Roh- Werkst 1999. https://doi.org/10.1007/s001070050040.
[31] Thommes M, Kaneko K, Neimark AV, Olivier JP, Rodriguez-Reinoso F, Rouquerol J, et al. Physisorption of gases, with special reference to the evaluation of surface area and pore size distribution (IUPAC Technical Report). Pure Appl Chem 2015;87(9–10):1051–69. https://doi.org/10.1515/pac-2014-1117.
[32] Xiao T, Yuan H, Ma Q, Guo X, Wu Y. An approach for in situ qualitative and quantitative analysis of moisture adsorption in nanogram-scaled lignin by using micro-FTIR spectroscopy and partial least squares regression. Int J Biol Macromol 2019. https://doi.org/10.1016/j.ijbiomac.2019.04.043.
[33] Schwanninger M, Rodrigues JC, Fackler K. A review of band assignments in near infrared spectra of wood and wood components. J Near Infrared Spectrosc 2011. https://doi.org/10.1255/jnirs.955.
[34] Mitsui K, Inagaki T, Tsuchikawa S. Monitoring of hydroxyl groups in wood during heat treatment using NIR spectroscopy. Biomacromolecules 2008. https://doi.org/10.1021/bm7008069.
[35] Workman JJ, Weyer L. Practical guide to interpretive near-infrared spectroscopy. 2007. https://doi.org/10.1201/9781420018318.
[36] Alves A, Santos A, Rozenberg P, Pâques LE, Charpentier JP, Schwanninger M, et al. A common near infrared-based partial least squares regression model for the prediction of wood density of Pinus pinaster and Larix × eurolepis. Wood Sci Technol 2012. https://doi.org/10.1007/s00226-010-0383-x.
[37] Inagaki T, Yonenobu H, Tsuchikawa S. Near-infrared spectroscopic monitoring of the water adsorption/desorption process in modern and archaeological wood. Appl Spectrosc 2008;62:860–5. https://doi.org/10.1366/000370208785284312.
[38] Watanabe A, Morita S, Ozaki Y. A study on water adsorption onto microcrystalline cellulose by near-infrared spectroscopy with two-dimensional correlation spectroscopy and principal component analysis. Appl Spectrosc 2006. https://doi.org/10.1366/000370206778397452.
[39] Pentrák M, Bizovská V, Madejová J. Near-IR study of water adsorption on acid-treated montmorillonite. Vib Spectrosc 2012. https://doi.org/10.1016/j.vibspec.2012.07.012.
[40] Fackler K, Schwanninger M. Polysaccharide degradation and lignin modification during brown rot of spruce wood: a polarised Fourier transform near infrared study. J Near Infrared Spectrosc 2010. https://doi.org/10.1255/jnirs.901.
[41] Barton FE, Himmelsbach DS. Two-dimensional vibrational spectroscopy II: correlation of the absorptions of lignins in the mid-and near-infrared. Appl Spectrosc 1993. https://doi.org/10.1366/0003702934066091.
[42] Michell AJ, Schimleck LR. NIR spectroscopy of woods from Eucalyptus globulus. 1996.
[43] Noda I. Advances in two-dimensional correlation spectroscopy. Vib Spectrosc 2004. https://doi.org/10.1016/j.vibspec.2003.12.016.